

Ryanodine Receptor Type 1 (RyR1) Mutations C4958S and C4961S Reveal Excitation-coupled Calcium Entry (ECCE) Is Independent of Sarcoplasmic Reticulum Store Depletion*

Received for publication, June 14, 2005, and in revised form, August 5, 2005. Published, JBC Papers in Press, August 24, 2005, DOI 10.1074/jbc.M506441200

Alanna M. Hurne^{†1}, Jennifer J. O'Brien^{‡1,2}, Douglas Wingrove^{¶1}, Gennady Cherednichenko[‡], Paul D. Allen[¶], Kurt G. Beam[§], and Isaac N. Pessah^{†‡3}

From the [†]Department of Molecular Biosciences, School of Veterinary Medicine and Center for Children's Environmental Health and Disease Prevention, University of California, Davis, California 95616, the [§]Department of Biomedical Sciences, Colorado State University, Fort Collins, Colorado 80523, and the [¶]Department of Anesthesia, Perioperative and Pain Medicine, Brigham and Women's Hospital, Boston, Massachusetts 02115

Bi-directional signaling between ryanodine receptor type 1 (RyR1) and dihydropyridine receptor (DHPR) in skeletal muscle serves as a prominent example of conformational coupling. Evidence for a physiological mechanism that upon depolarization of myotubes tightly couples three calcium channels, DHPR, RyR1, and a Ca²⁺ entry channel with SOCC-like properties, has recently been presented (Cherednichenko, G., Hurne, A. M., Fessenden, J. D., Lee, E. H., Allen, P. D., Beam, K. G., and Pessah, I. N. (2004) *Proc. Natl. Acad. Sci. U. S. A.* 101, 15793–15798). This form of conformational coupling, termed excitation-coupled calcium entry (ECCE) is triggered by the α_{1S} -DHPR voltage sensor and is highly dependent on RyR1 conformation. In this report, we substitute RyR1 cysteines 4958 or 4961 within the TXCFICG motif, common to all ER/SR Ca²⁺ channels, with serine. When expressed in skeletal myotubes, C4958S- and C4961S-RyR1 properly target and restore L-type current via the DHPR. However, these mutants do not respond to RyR activators and do not support skeletal type EC coupling. Nonetheless, depolarization of cells expressing C4958S- or C4961S-RyR1 triggers calcium entry via ECCE that resembles that for wild-type RyR1, except for substantially slowed inactivation and deactivation kinetics. ECCE in these cells is completely independent of store depletion, displays a cation selectivity of Ca²⁺ > Sr²⁺ ~ Ba²⁺, and is fully inhibited by SKF-96365 or 2-APB. Mutation of other non-CXXC motif cysteines within the RyR1 transmembrane assembly (C3635S, C4876S, and C4882S) did not replicate the phenotype observed with C4958S- and C4961S-RyR1. This study demonstrates the essential role of Cys⁴⁹⁵⁸ and Cys⁴⁹⁶¹ within an invariant CXXC motif for stabilizing conformations of RyR1 that influence both its function as a release channel and its interaction with ECCE channels.

Calcium is a universal intracellular signal responsible for regulating many cellular processes including cell proliferation, hormonal secretion, and muscle contraction (1, 2). Most eukaryotic cells generate spatially and temporally encoded intracellular signals through the coordi-

nated release of Ca²⁺ from endoplasmic reticulum (ER)⁴/sarcoplasmic reticulum (SR) stores and by extracellular Ca²⁺ entry across the plasma membrane. Inositol 1,4,5-trisphosphate receptors (IP₃Rs) and ryanodine receptors (RyRs) dynamically control the release of Ca²⁺ from intracellular stores. In addition, there is evidence showing conformational coupling between RyRs and L-type voltage-gated Ca²⁺ channels (DHPR; Refs. 3 and 4; store-operated Ca²⁺ channels (SOCCs; Ref. 5), or Ca²⁺-activated K⁺-channels (6, 7). SOCCs are essential calcium entry pathways for regulating Ca²⁺ signals and replenishing ER/SR stores of both nonexcitable and excitable cells (8–10). Several theories have been proposed to account for the activation of store-operated Ca²⁺ entry (SOCE), including the involvement of a diffusible second messenger (11) and rapid vesicular translocation (12, 13). Ca²⁺ entry pathways evoked by physiological stimulation of phosphatidylinositol 4,5-bisphosphate or elements of the DAG limb of the phosphoinositide pathway such as arachidonate also appear to directly modulate Ca²⁺ entry by a mechanism that is independent of store depletion (14, 15). Evidence for the conformational coupling hypothesis, whereby activation of Ca²⁺ entry is tightly coupled to changes in the conformation of RyRs and IP₃Rs, has also been provided in both non-excitable and excitable cells (5, 16–20).

In skeletal muscle, a specialized form of conformational coupling occurs between DHPR and RyR1. Skeletal excitation-contraction (EC) coupling (an orthograde signal from DHPR to RyR1) results in release of Ca²⁺ from the SR without a requirement for entry of extracellular Ca²⁺. Additionally, a retrograde signal from RyR1 to the DHPR regulates the magnitude of the inward Ca²⁺ current carried by the DHPR (3, 21–24). Block of RyR1 with micromolar ryanodine causes a substantial (2-nm) shift in the relative positions of the four DHPRs within each tetrad, indicating that ryanodine induces large conformational changes in the RyR1 cytoplasmic domain and that the α_{1S} -DHPR-RyR1 complex acts as a physically coupled unit (25). Within the DHPR, a 45-amino acid stretch of the α_{1S} II-III loop (corresponding to Leu⁷²⁰-Leu⁷⁶⁴) and the C-terminal of β_{1a} are both important for bi-directional signaling (26), and several regions of RyR1 are important for interacting with the DHPR (27–29). In addition to bi-directional signaling engaged during EC coupling, there are Ca²⁺ entry mechanisms involving yet unidentified SOCC in muscle cells (see Ref. 30, for review). The activation of SOCC in myotubes has been linked to two distinct mechanisms. One

* This work was supported by National Institutes of Health Grants 2P0 AR17605, 1P0 ES11269, and 2R01 AR43140. The costs of publication of this article were defrayed in part by the payment of page charges. This article must therefore be hereby marked "advertisement" in accordance with 18 U.S.C. Section 1734 solely to indicate this fact.

¹ Both authors made equal contributions to this work.

² Present address: Dept. of Pharmacology, University of Washington, Seattle, WA 98195.

³ To whom correspondence should be addressed: Dept. of VM:Molecular Biosciences, University of California, Davis, CA 95616. Tel.: 530-752-6696; Fax: 530-752-4698; Email: inpessah@ucdavis.edu.

⁴ The abbreviations used are: ER, endoplasmic reticulum; RyR, ryanodine receptor; DMEM, Dulbecco's modified Eagle's medium; EC, excitation-contraction; ECCE, excitation-coupled calcium entry; SOCE, store-operated Ca²⁺ entry; CPA, cyclopiazonic acid; SR, sarcoplasmic reticulum; DHPR, dihydropyridine receptor; CmC, 4-chloro-m-cresol; CPM, 7-diethylamino-3-(4'-maleimidylphenyl)-4-methylcoumarin.

form of Ca^{2+} entry, unmasked in the presence of the SERCA pump blockers thapsigargin (TG) (31) or cyclopiazonic acid (32) is activated subsequent to chronic store depletion and appears to be closely related to SOCE commonly described in non-excitable cells. A second mechanism, termed excitation-coupled Ca^{2+} entry (ECCE) was recently described in skeletal myotubes (33). Unlike SOCE, the expression of both α_{1S} -DHPR and RyR1 are essential for engaging ECCE. ECCE is triggered by membrane depolarization, whereas SOCE is inhibited by membrane depolarization (17). α_{1S} -DHPR serves as the voltage sensor for triggering the activation of ECCE, and the conformational state of RyR1 dramatically influences the behavior of ECCE in response to membrane depolarization. For example, the fully blocked RyR1 conformation assumed in the presence of micromolar ryanodine significantly slows the inactivation of the ECCE during a maintained depolarization (33). Initial experiments with ryanodine-treated myotubes indicate that ECCE, unlike SOCE, does not appear to depend on appreciable depletion of SR stores to be fully engaged.

Elements of structure within RyR1 important for regulating either ECCE or SOCE are not known. Cysteine residues are integral for inducing and maintaining the three-dimensional conformation in proteins by forming critical inter- and intramolecular disulfide bond linkages. The RyR is known to contain several classes of cysteine residues with different chemical reactivities. Much attention has been focused on the role of extremely reactive cysteine residues as key structural components contributing to redox modulation and nitrosylation of the channel complex (see Refs. 34 and 35). Recently seven hyper-reactive cysteines of RyR1, including the nitrosylation site Cys³⁶³⁵, were identified using chemical labeling and mass spectroscopic techniques (36). Located in the cytoplasmic tail of all RyR and IP₃R isoforms is a highly conserved TXCFICG motif with two invariant cysteine residues (Cys⁴⁹⁵⁸ and Cys⁴⁹⁶¹ in RyR1). Although this motif conforms to the CXXC consensus known to confer redox sensitivity to thiol/disulfide oxidoreductases (37), the contribution of Cys⁴⁹⁵⁸ and Cys⁴⁹⁶¹ to RyR1 conformation and function are unknown.

In the present study, we report that two mutated RyR1s (C4958S or C4961S) target properly to junctions after expression in 1B5 or primary myotubes, as indicated by the restoration of retrograde signaling to the α_{1S} -DHPR. However, cells expressing these proteins lack EC coupling because the mutant release channels fail to activate, even in response to direct agonists. Nonetheless, C4958S- and C4961S-RyR1 maintain their ability to engage ECCE, which demonstrates that ECCE occurs in the absence of SR store depletion that would result from SR Ca^{2+} release. Interestingly, the inactivation of ECCE with C4958S- or C4961S-RyR1 is substantially slower than with wild-type RyR1. These data further differentiate ECCE from classic SOCE and show that cysteines 4958 and 4961 near the C terminus function both to maintain conformations necessary for RyR1 channel function and to influence conformational activation of ECCE.

EXPERIMENTAL PROCEDURES

cDNA Cloning—Cys⁴⁹⁵⁸ and Cys⁴⁹⁶¹ were mutated to serine using primer extension-driven site-directed mutagenesis in a ClaI(14,203)-XbaI (vector) fragment of RyR1 using a QuikChange® (Stratagene, CA) kit, and sequenced in both directions to confirm the mutation and the absence of any other random mutations. The primers used to create either mutation (note: mutated sequence is indicated in lowercase) are: forward 5'-GAGACAAAa/tGCTTCATCa/tGCCGGATTG-3', reverse 5'-CTCTGGTTTt/aCGAAGTAGt/aCGCCCTAAC-3' with the first substitution yielding C4958S and the second yielding C4961S. The mutated fragments were then ligated back into the full-length RyR1

constructs in pHSVprPUC HSV amplicon vector (38) or into both the pCDNA3 and the pCI-neo mammalian expression vectors (39). A similar method was used to create the C3635S, C4876S, and C4882S mutations.

Culture of 1B5 and Primary Mouse Skeletal Myotubes—1B5 myogenic cells (40) were cultured in Dulbecco's modified Eagles medium (DMEM) containing 20% (v/v) fetal bovine serum, 2 mM L-glutamine, 100 units/ml penicillin-G, and 0.1 $\mu\text{g}/\text{ml}$ streptomycin sulfate (Invitrogen, Life Technologies, Inc.) at 37 °C in 10% CO_2 , 5% O_2 . For Fura-2 ratio fluorescence imaging measurements, cells were grown on collagen (calf skin; Calbiochem) coated 72-well polystyrene plates (Nalge Nunc International, Rochester, NY) or 96-well μ -clear plates (Greiner, Frederick, MD). Once dividing cells were ~50% confluent, they were stimulated to differentiate into myotubes over a period of 6–8 days in growth factor-deprived medium consisting of DMEM containing 2% (v/v) heat-inactivated horse serum (HIHS), 2 mM L-glutamine, 100 units/ml penicillin-G, and 0.1 $\mu\text{g}/\text{ml}$ streptomycin sulfate at 37 °C in 10% CO_2 , 10% O_2 .

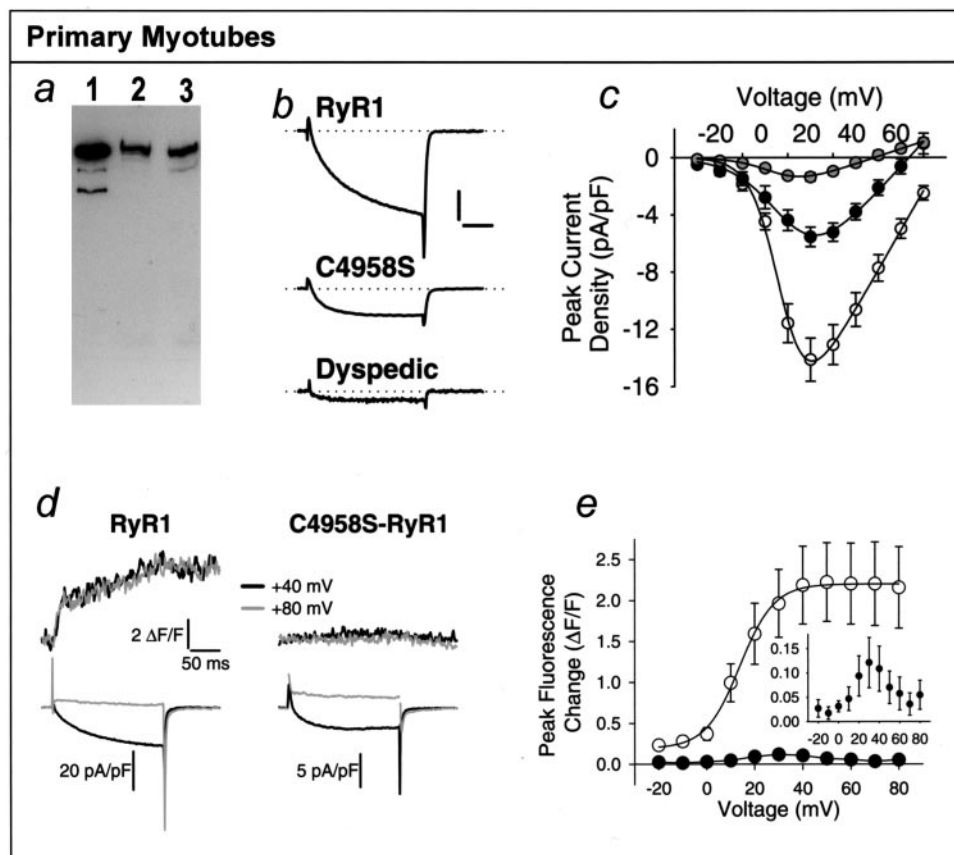
Preparation of primary cultures of skeletal myotubes from wild-type and dyspedic (lacking RyR1) mice has been described previously (41). Wild-type and dyspedic primary myoblasts were grown on 100-mm tissue culture-treated Corning dishes and cultured in Ham's F-10 nutrient medium containing 20% (v/v) fetal bovine serum, 2 mM L-glutamine, 5 ng/ml fibroblast growth factor (rhFGF; Promega, Madison, WI), 100 units/ml penicillin-G, and 0.1 $\mu\text{g}/\text{ml}$ streptomycin sulfate at 37 °C in 10% CO_2 , 5% O_2 . For Fura-2 imaging cells were plated onto 96-well μ -clear plates (Greiner) coated with MATRIGEL (BD Biosciences) or collagen. Upon reaching ~80% confluence, the cells were differentiated into myotubes over a period of 3–5 days using DMEM containing 2% (v/v) HIHS, 2 mM L-glutamine, 100 units/ml penicillin-G, and 0.1 $\mu\text{g}/\text{ml}$ streptomycin sulfate at 37 °C in 10% CO_2 , 10% O_2 .

Transduction of Skeletal Myotubes with cDNAs—For Ca^{2+} -imaging studies, differentiated 1B5 and primary dyspedic myotubes were transduced with helper virus-free herpes simplex virus-1 amplicon viruses (1×10^5 to 3×10^5 infectious units/ml) (38) containing the cDNA encoding for either wild-type RyR1, C4958S- or C4961S-RyR1 in antibiotic-free DMEM containing 2% HIHS for 1 h at 37 °C, 10% CO_2 , 10% O_2 . After 1 h, the virus-containing medium was replaced with differentiation medium, and the cells were used for imaging experiments 24–48 h post-transduction.

For measurement of whole cell currents, a single nucleus of each myotube (6–7 days after initial plating) was microinjected with 0.3 $\mu\text{g}/\mu\text{l}$ of either C4958S-, or C4961S-RyR1 pCDNA3 or RyR1-pCI-neo and 0.2 $\mu\text{g}/\mu\text{l}$ of an expression plasmid (42) for the surface antigen CD8. Approximately 48 h later, the medium was removed from injected myotubes and replaced with external recording solution (see below) containing beads coated with CD8 antibody (Dynabeads M-450, Dynal AS, Oslo, Norway), which allowed identification of cells that were expressing CD8, and thus candidates to express the RyR construct of interest. Alternatively, the RyR cDNA was injected together with 0.04 $\mu\text{g}/\mu\text{l}$ cDNA for green fluorescent protein (43). After 48 h, the CD8- or GFP-positive myotubes were used for experiments.

Whole Cell Measurements of Ca^{2+} Currents and Transients—The whole cell technique was used for the simultaneous measurement of Ca^{2+} currents and transients (44). Patch pipettes were pulled from borosilicate glass and had resistances of 1.6–2.0 M Ω when filled with internal solution, which contained (in mM) 145 cesium glutamate, 8 MgATP (1 mM free Mg^{2+}), 2 CsCl, 10 HEPES, 10 EGTA, and 0.5 K₃Fluo-3 (Molecular Probes, Eugene, OR) as the Ca^{2+} indicator. After a seal was obtained between the patch pipette and a myotube, bath per-

FIGURE 1. RyR1 point mutant C4958S restores L-type Ca^{2+} current, but not EC coupling, in primary dyspedic myotubes. *a*, Western blot analysis of 1B5 myotubes virally transduced with C4958S-RyR1 (lane 2; 20 μg of protein) or wild-type RyR1 (lane 3; 20 μg of protein). Lane 1 shows 0.5 μg of rabbit junctional SR protein as control. *b*, representative Ca^{2+} currents at +30 mV from dyspedic myotubes expressing wild-type RyR1 (top) and C4958S-RyR1 (middle), and from uninjected dyspedic myotubes (bottom). The vertical and horizontal scale bars represent 5 pA/pF and 50 ms, respectively. *c*, peak Ca^{2+} current-voltage relationships of dyspedic myotubes (gray circles; $n = 10$), C4958S-RyR1 expressing myotubes (black circles; $n = 32$), and wild-type RyR1 expressing myotubes (white circles; $n = 41$). *d*, representative Ca^{2+} transients at +40 mV (black) and +80 mV (gray) for wild-type RyR1 and C4958S-RyR1. *e*, peak Ca^{2+} -induced fluorescence increase in myotubes expressing wild-type RyR1 (white circles; $n = 12$) or C4958S-RyR1 (black circles; $n = 8$) is plotted against test potential. The inset is an enlargement of the C4958S-RyR1 data to emphasize the bell shape of the voltage dependence.



fusion was used to remove any indicator that had leaked from the pipette. A period of >5 min was allowed after breaking into whole cell mode so that Fluo-3 could diffuse throughout the myotube. Ca^{2+} currents were measured with a Warner PC501 patch amplifier (Hamden, CT) and transients with a photomultiplier apparatus (Biomedical Instrumentation Group, University of Pennsylvania, Philadelphia, PA). Cells were held at -80 mV and control (linear capacitive and leak) currents were measured by steps to -110 mV. Cell capacitance was determined by integration of the control current and used to normalize Ca^{2+} currents (pA/pF). Additionally, the average of 10 control currents was digitally scaled and subtracted from test currents to correct for linear components of leakage and capacitive current. The voltage protocol for test currents consisted of a 1-s prepulse to -30 or -20 mV to inactivate T-type current, followed by a 50-ms repolarization to -50 mV, followed by a 200-ms step to the test potential, a 125-ms step to -50 mV, and finally a return to the holding potential. The external solution used for measuring Ca^{2+} currents contained (in mM) 145 TEACl, 10 HEPES, 10 CaCl_2 , and 0.003 TTX.

To measure responses to application of cyclopiazonic acid (CPA), intact cells were loaded with Fluo3-AM as described previously (44). Fluorescence data were recorded by applying 1-s fluorescence excitation pulses at 0.1 Hz and averaging the fluorescent emission during a 200–800-ms interval centered within each excitation pulse. Baseline fluorescence (F) was determined prior to the application of CPA and used to calculate the normalized change in fluorescence, $\Delta F/F$. Response latency was determined as the time from application of CPA until the first data point exceeding the baseline by greater than two standard deviations. The effects of CPA, which was applied in rodent Ringer containing (mM) 145 NaCl, 5 KCl, 2 CaCl_2 , 1 MgCl_2 , 10 HEPES (pH 7.4 with NaOH), were tested on only a single myotube per culture dish.

Ca^{2+} and Mn^{2+} Imaging—Differentiated 1B5 or primary myotubes were loaded with the Ca^{2+} -sensitive dye Fura-2-AM (5 μM) at 37 °C for 20 min in imaging buffer (in mM) 125 NaCl, 5 KCl, 2 CaCl_2 , 1.2 MgSO_4 , 6 dextrose, and 25 HEPES, pH 7.4 supplemented with 0.05% bovine serum albumin. The cells were then washed with imaging buffer supplemented with 250 μM sulfonpyrazone and transferred to a Nikon Diaphot microscope. Fura-2 was excited alternatively at 340 and 380 nm, using a Delta Ram excitation source and fluorescence images magnified with $\times 10$ or $\times 40$ objectives were detected at 510 nm with an IC-300 ICCD camera (Photon Technology International; PTI, Lawrenceville, NJ). Images were captured, digitized, and stored on computer using ImageMaster software (PTI). Ratiometric (340/380) data were collected from regions of 5 to 15 individual cells. Agonists were dissolved in imaging buffer and perfused into wells containing the myotubes. When high KCl concentrations were used (>40 mM), the concentration of Na^+ was lowered accordingly to preserve osmolarity. In some experiments the chloride product was kept constant by substitution of potassium methane sulfonate, and was not found to influence the myotube parameters measured in the present study.

In some experiments, the manganese quench method was employed (45–47). Mn^{2+} enters the cell through plasma membrane channels but cannot be removed via the ATPase pumps. After loading the cells with Fura-2-AM the extracellular solution was replaced with Ca^{2+} -free imaging buffer containing a final concentration of 0.5 mM Mn^{2+} . Fura-2 was excited at 360 nm and emission measured at 510 nm with a $\times 10$ or $\times 40$ objective. After recording a baseline decrease in fluorescence intensity (due to Mn^{2+} quenching the dye), cells were then depolarized with KCl and the new rate of quench observed. For electrical field stimulation, two platinum electrodes were fixed to opposite sides of the well and connected to an AMPI Master 8 stimulator. Myotubes were loaded with Fura-2 and stimulated with 25-ms, 6-V pulses over a range of

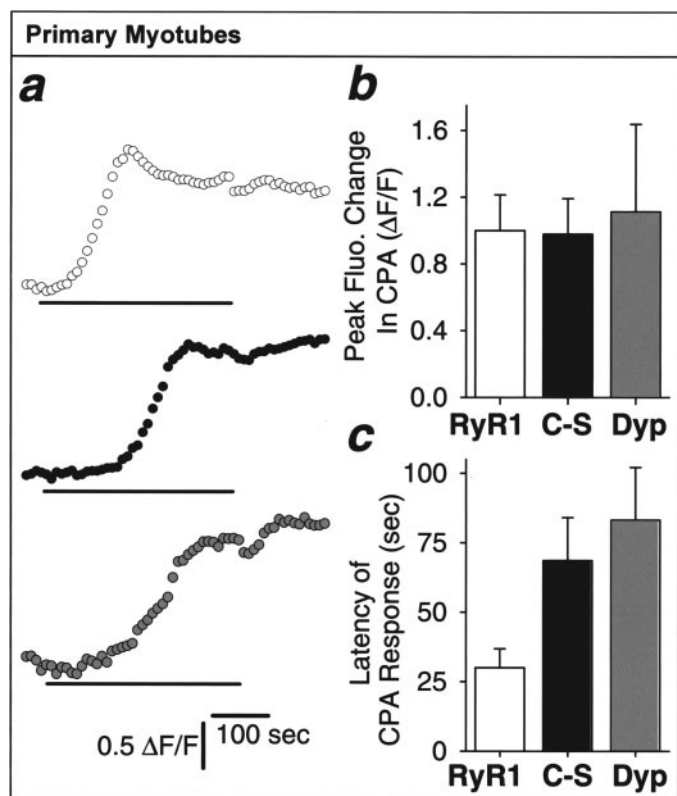


FIGURE 2. SR Ca^{2+} stores are similar in myotubes expressing wild-type or C4958S-RyR1 and in dyspedic myotubes. *a*, changes in Fluo3 fluorescence in intact, primary myotubes expressing wild-type RyR1 (white circles) or C4958S-RyR1 (black circles), and in uninjected dyspedic (gray circles) in response to bath application of $30 \mu\text{M}$ CPA. *b*, average, normalized peak fluorescence increases during exposure to $30 \mu\text{M}$ CPA for C4958S-RyR1 (C-S, black bars; $n = 8$), wild-type RyR1 (white bars; $n = 6$), and dyspedic myotubes (Dyp, gray bars; $n = 7$). *c*, the latency between the application of CPA and the first detectable increase in fluorescence for wild-type RyR1 (white bars; $n = 6$), C4958S-RyR1 (C-S, black bars; $n = 7$), and dyspedic myotubes (Dyp, gray bars; $n = 6$).

frequencies (5–20 Hz). In these experiments, data were acquired at 50-ms intervals by photometry.

Sarcoplasmic Reticulum Membrane Preparation—Differentiated myotubes transfected with virions containing the cDNA encoding for C4958S and wild-type RyR1 were washed with ice-cold PBS and scraped off 100-mm plates using 3 ml of cold harvest buffer (in mM: 137 NaCl, 3 KCl, 8 Na_2HPO_4 , 1.5 KH_2PO_4 , 0.5 Na_4EDTA at pH 7.4) and centrifuged at $500 \times g$ for 5 min. The cell pellet was resuspended in ice-cold hypotonic lysis buffer (1 mM EDTA, 5 μM leupeptin, 250 μM phenylmethylsulfonyl fluoride, 10 mM HEPES at pH 7.4) and homogenized on ice using a PowerGen 700D homogenizer (Fisher Scientific) for 3×5 s at 14,000 rpm. An equal volume of ice-cold 20% sucrose buffer (10 mM HEPES, pH 7.4) was added and the homogenization process repeated. The homogenate was ultracentrifuged at 33,000 rpm for 1 h, at 4°C in a Ti80 rotor and the crude pellet resuspended in 10% sucrose-HEPES buffer solution, aliquoted, and stored at -80°C .

Western Blot Analysis—Proteins were denatured in 1:1 in a solution containing 10% mercaptoethanol and 10% sucrose-HEPES buffer for 30 min at 60°C before being loaded onto a 3–10% gradient sodium dodecyl sulfate-polyacrylamide gel and subjected to electrophoresis at 200 V for 45 min. The size-separated proteins were then transferred slowly onto polyvinylidene difluoride microporous membranes (Millipore, Bedford, MA) using an electroblotter (Mini Transblot; Bio-Rad) for 16 h at 200 V followed by a rapid transfer for 1 h at 100 V. The transferred proteins were then incubated in TTBS buffer (20 mM Tris base, 137 mM NaCl, 0.05% Tween 20, pH 7.4) containing 5% nonfat dry milk at ambient

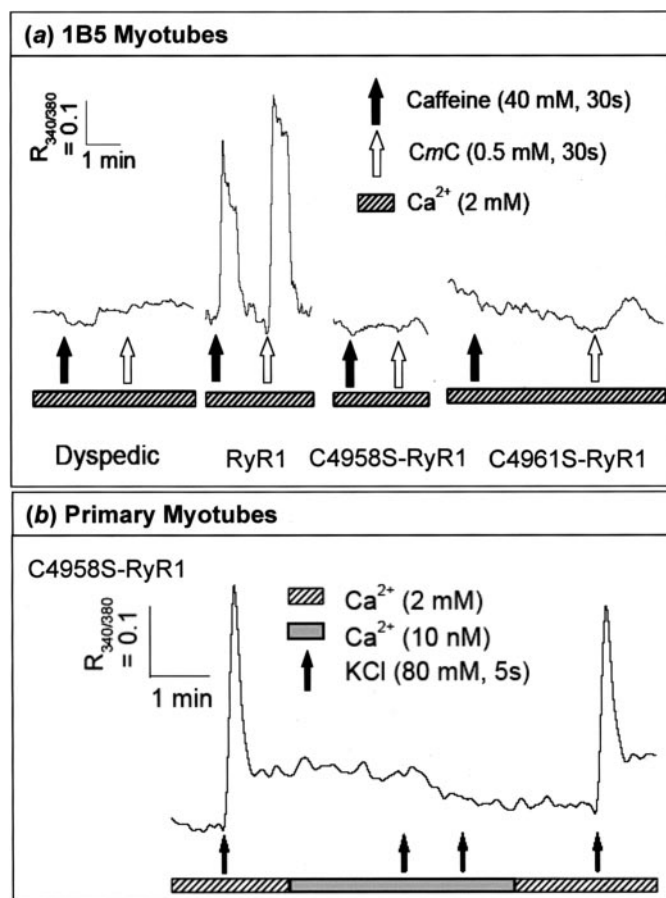


FIGURE 3. RyR1 Cys point mutants (C4958S and C4961S) expressed in dyspedic myotubes are unresponsive to direct RyR agonists but engage Ca^{2+} entry. *a*, representative responses are shown for caffeine and CmC applied to 1B5 dyspedic myotubes ($n = 175$ cells), and 1B5 myotube expressing wild-type RyR1 (RyR1; $n = 617$ cells), C4958S-RyR1 ($n = 738$ cells), or C4961S-RyR1 ($n = 208$ cells). *b*, representative response to depolarization of primary myotubes expressing C4958S-RyR1 in the presence and absence of physiological concentration of external Ca^{2+} in the medium ($n = 25$ cells). Primary myotubes ($n = 32$ cells) also failed to respond to either caffeine or CmC (data not shown).

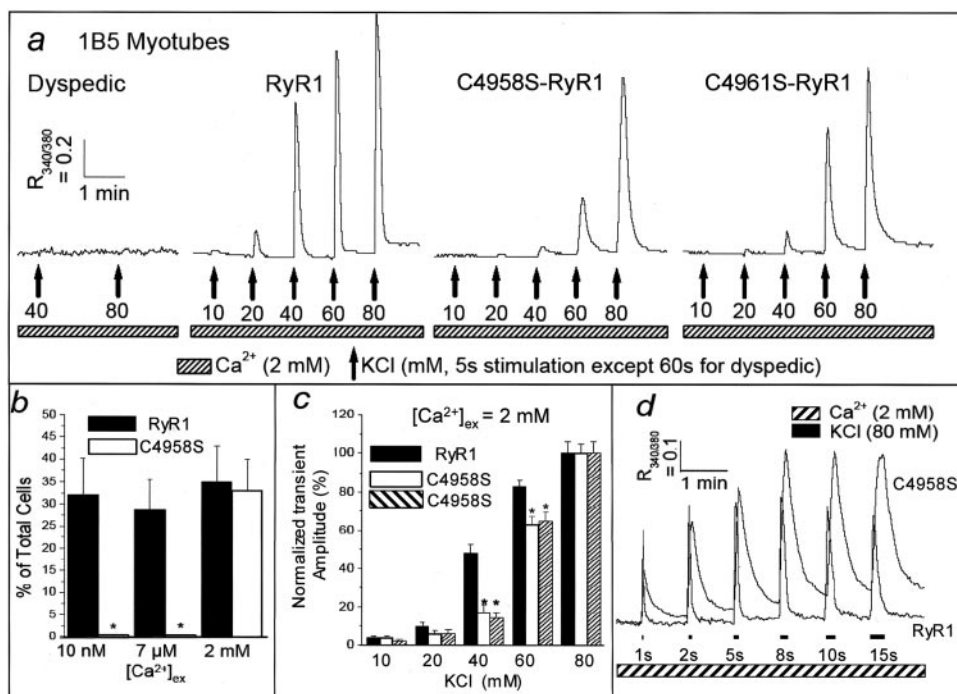
temperature for 30 min. The blot was then probed with 34C primary antibody (1:200 dilution; Developmental Studies Hybridoma Bank, Iowa City, IA; Refs. 23 and 71) diluted 200 times in TTBS buffer plus 1% bovine serum albumin at 25°C . After 1 h the blot was rinsed in TTBS buffer three times and then incubated with the secondary antibody (goat anti-rabbit IgG at a 1:20,000 dilution) for 1 h at 25°C . After a final rinse step with TTBS, enhanced chemiluminescence techniques (PerkinElmer Life Science Products) were used to visualize the immunoblots.

RESULTS

C4958S-RyR1 Enhances L-type Ca^{2+} Current, but Lacks EC Coupling—Western analysis of homogenates from myotubes expressing C4958S- or wild-type RyR1 revealed the presence of one predominant immunoreactive band whose size was indistinguishable from that of junctional SR from adult rabbit (Fig. 1*a*). Similar results were obtained with preparations of C4961S-RyR1 (not shown). Additional immunocytochemical labeling experiments not shown here indicated that C4958S- or wild-type RyR1 were distributed within expressing myotubes in punctate rows, consistent with localization to Ca^{2+} release units at surface membrane/SR junctions (48).

The processing and targeting of C4958S-RyR1 were functionally tested by whole cell voltage clamp after expression in primary dyspedic myotubes. In agreement with previous results (3), the expression of

FIGURE 4. Depolarization triggers Ca^{2+} entry in myotubes expressing C4958S- or C4961S-RyR1. *a*, representative traces of the functional responses of dyspedic 1B5 myotubes, ($n = 33$ cells) and of 1B5 myotubes expressing wild-type RyR1 (RyR1); ($n = 30$ cells); C4958S-RyR1 ($n = 35$ cells); and C4961S-RyR1 ($n = 34$ cells) after stimulation (5 s) with 10, 20, 40, 60, and 80 mM KCl. *b*, summary data of the effect of $[\text{Ca}^{2+}]_{\text{ex}}$ on the response induced by 80 mM KCl in C4958S-RyR1 ($n = 89$ cells) and wild-type RyR1 ($n = 89$ cells) 1B5 myotubes. The calcium responses observed in the absence of extracellular calcium for C4958S (*, $p < 0.001$) were significantly different to that observed in the presence of calcium. *c*, the functional responses (measured in terms of relative changes in $[\text{Ca}^{2+}]_{\text{ex}}$) of wild-type RyR1 ($n = 11$ cells), C4958S-RyR1 ($n = 14$ cells), and C4961S-RyR1 ($n = 13$ cells) to varying concentrations of K^+ in the presence of 2 mM extracellular Ca^{2+} . The responses observed with C4958S- and C4961S-RyR1 at 40 and 60 mM K^+ are significantly less (*, $p < 0.036$) than those observed with wild-type RyR1-transfected 1B5 cells at the respective concentrations. *d*, representative traces of the functional responses of wild-type RyR1 ($n = 36$ cells) and C4958S-RyR1 ($n = 38$ cells) transduced 1B5 myotubes after stimulation for 1, 2, 5, 8, 10, and 15 s with 80 mM KCl in the presence of 2 mM external calcium.



wild-type RyR1 greatly enhanced peak L-type Ca^{2+} current density compared with dyspedic myotubes (-14.1 ± 1.5 versus -1.4 ± 0.3 pA/pF; Fig. 1, *b* and *c*). The wild-type RyR1 also restored skeletal-type EC coupling in that (i) the depolarization-induced calcium transient was of comparable size at +40 and +80 mV despite large differences in the size of the L-type Ca^{2+} current (Fig. 1*d*) and (ii) the amplitude of the transient displayed a sigmoid dependence on test potential (Fig. 1*e*). Like wild-type RyR1, C4958S-RyR1 enhanced peak L-type Ca^{2+} current (Fig. 1, *b* and *c*), although to a lesser extent (-5.5 ± 0.7 versus -14.1 pA/pF ± 1.5). This enhancement of current supports the idea that C4958S-RyR1 interacts with the DHPR as a consequence of targeting to SR junctions with the plasma membrane.

Unlike wild-type RyR1, however, expression of 4958S-RyR1 failed to restore skeletal type EC coupling. Although depolarization-induced transients were sometimes observed, they appeared to reflect Ca^{2+} entry via the DHPR because they were absent at +80 mV (Fig. 1*d*), were of small amplitude, and showed a bell-shaped dependence on test potential (Fig. 1*e*). To test whether a lack of SR Ca^{2+} stores was responsible for this absence of skeletal-type EC coupling, the filling state of the stores were assessed by exposing intact myotubes to the SERCA pump blocker CPA. The resulting increase in cytoplasmic Ca^{2+} had a similar magnitude in myotubes expressing wild-type RyR1, myotubes expressing C4956S-RyR1 and in control dyspedic myotubes (Fig. 2, *a* and *b*), suggesting that SR Ca^{2+} content was similar in the three types of cells. Comparable results were obtained when 200 nM thapsigargin was applied in an external solution containing 10 nM Ca^{2+} to 1B5 myotubes expressing wild-type or C4958S-RyR1 (data not shown). The latency of the response to CPA in myotubes expressing wild-type RyR1 was about 2-fold shorter than in dyspedic myotubes and C4958S-RyR1-expressing myotubes (Fig. 2*c*), most likely because RyR1 channels capable of active release accelerated the loss of Ca^{2+} from the SR. Myotubes expressing C4961S-RyR1 exhibited L-type Ca^{2+} currents and lack of EC coupling that were indistinguishable from those described for C4958S-RyR1 (data not shown).

ECCE in Myotubes Expressing C4958S- or C4961S-RyR1—Dyspedic 1B5 myotubes have been shown to lack detectible expression of any of

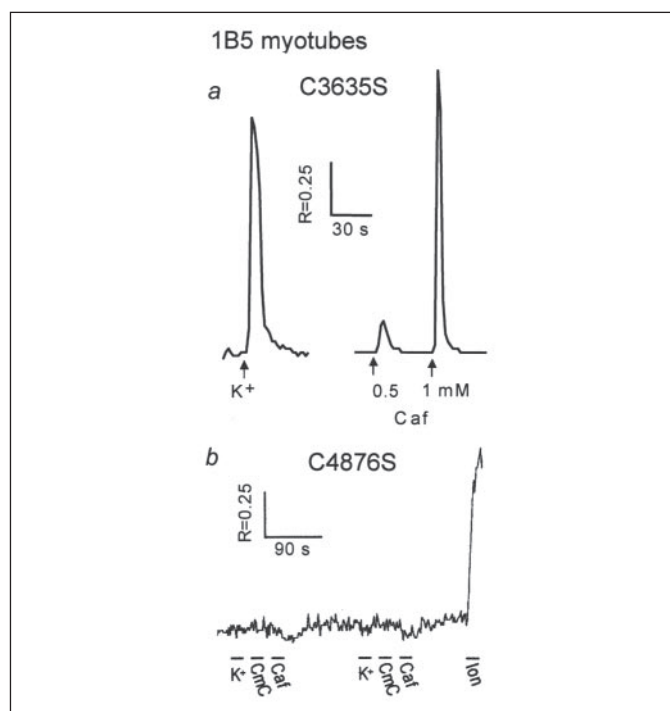


FIGURE 5. C3635S- and C4876S-RyR1 do not produce the same phenotype as CXXC mutants. Dyspedic 1B5 myotubes were transduced with cDNA to express C3635S- (*a*) or C4876S-RyR1 (*b*) mutations. Cells expressing C3635S-RyR1 responded to both depolarization by a brief (2 s) pulse of K^+ (40 mM) and to caffeine in a dose-dependent manner. By contrast cells expressing C4876S-RyR1 did not respond to K^+ , caffeine, or Cm (20 μM). Cells did respond to the Ca^{2+} ionophore ionomycin (Iom; 2 μM). Expression of RyR1 protein was verified by immunocytochemical staining with monoclonal antibody 34C (not shown). Data shown are a representative trace from at least $n = 5$ cells for each experiment.

the RyR isoforms but to express all of the other proteins essential for skeletal EC coupling (40). As expected, transduction of dyspedic 1B5 myotubes with wild-type RyR1 cDNA restored intracellular Ca^{2+} responses to direct activators caffeine and 4-chloro-*m*-cresol (CmC)

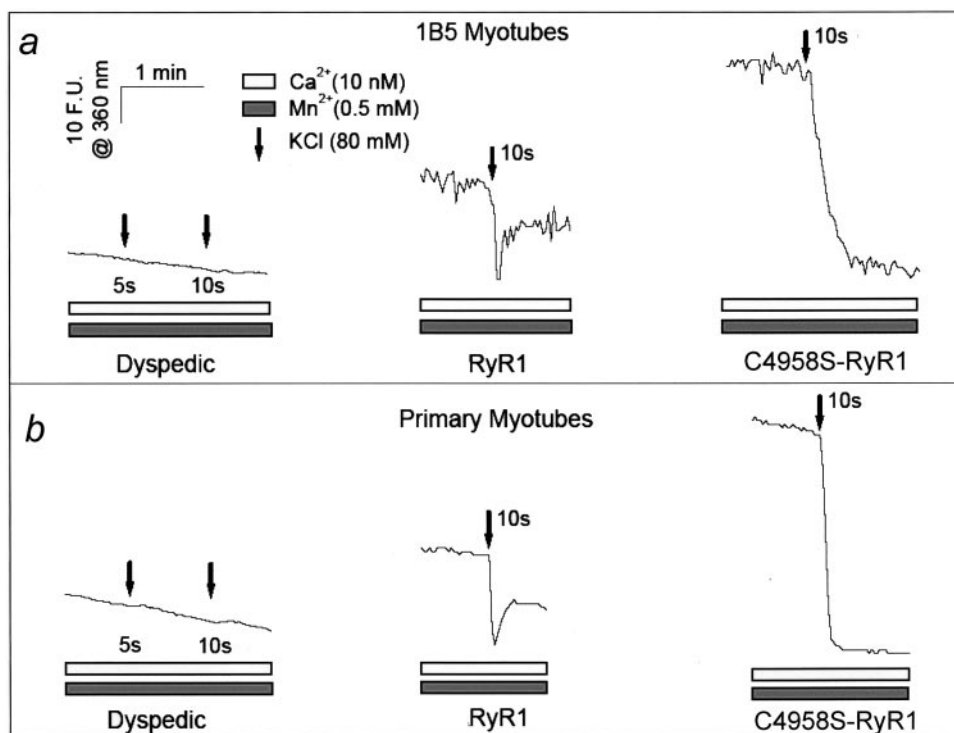


FIGURE 6. K^+ depolarization induces Mn^{2+} entry in 1B5 and primary myotubes. Representative traces are shown for 1B5 (a) and primary (b) myotubes. Depolarization with 80 mM KCl did not cause detectable quench of Fura-2 in dyspedic 1B5 (a, $n = 40$ cells) or primary myotubes (b, $n = 35$ cells). However, depolarization resulted in Mn^{2+} entry in wild-type RyR1-expressing 1B5 (a, $n = 36$ cells) or primary myotubes (b, $n = 45$ cells), as well as in C4958S-RyR1 expressing 1B5 (a, $n = 41$ cells) or primary myotubes (b, $n = 32$ cells). In the cells expressing wild-type RyR1, the Mn^{2+} -quench signal may have been partially obscured by a Fura-2 response to Ca^{2+} release as a consequence of skeletal-type EC coupling.

(Fig. 3), but 1B5 myotubes expressing C4958S- or C4961S-RyR1 failed to respond to either agonist (Fig. 3). Like 1B5 cells, primary myotubes expressing the cysteine mutant also failed to respond to these concentrations of caffeine or *CmC* (data not shown). However primary myotubes (Fig. 3b) and 1B5 myotubes (Fig. 4a) expressing the mutant RyRs responded vigorously to depolarization elicited by addition of 80 mM K^+ to the external medium with a large Ca^{2+} transient not seen in the absence of external Ca^{2+} (Fig. 3b).

Depolarization-triggered Ca^{2+} entry was further studied with 1B5 myotubes. Untransduced 1B5 myotubes failed to respond to a 60 s depolarization elicited by addition of 40 or 80 mM K^+ to the external medium (Fig. 4a, 1st trace), whereas myotubes expressing wild-type RyR1 responded to depolarization with a Ca^{2+} transient both in the presence ($[Ca^{2+}]_{ex} = 2$ mM; Fig. 4a, 2nd trace) and absence ($[Ca^{2+}]_{ex} = 10$ nM and 7μ M; Fig. 4b, black bars) of extracellular Ca^{2+} , consistent with restoration of skeletal type EC coupling. Like primary myotubes, 1B5 myotubes expressing either C4958S- or C4961S-RyR1 responded with a robust Ca^{2+} transient to K^+ depolarization (Fig. 4a, 3rd and 4th traces). However this depolarization-induced Ca^{2+} transient could be completely abolished by removal of Ca^{2+} from the external medium indicating that it was dependent on sarcolemmal Ca^{2+} entry (Fig. 4b, open bars; data for C4958S-RyR1 shown). The magnitude of depolarization-triggered Ca^{2+} response observed with C4958S- or C4961S-RyR1 expressing myotubes was dependent on the degree of depolarization (*i.e.* the external K^+ concentration), and cells expressing either mutant appeared to have a higher threshold for their response to depolarization than that needed to trigger EC coupling in myotubes expressing wild-type RyR1 (Fig. 4, a and c). The increase in intracellular Ca^{2+} observed with C4958S-RyR1-expressing cells differed from that in cells expressing wild-type RyR1 in that it rose more slowly, declined much less during the depolarizing stimulus, and decayed more slowly after K^+ was removed (Fig. 4d). Collectively, these data show that although substitution of Cys⁴⁹⁵⁸ or Cys⁴⁹⁶¹ with serine produces RyR1 channels that cannot be activated to produce Ca^{2+} release from the SR, these proteins target to junctions

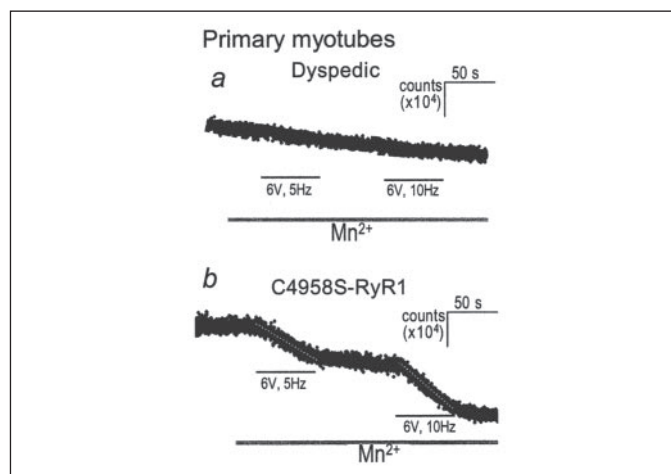


FIGURE 7. Electrical pulse trains rapidly enhance Mn^{2+} entry in primary myotubes expressing C4958S. Mn^{2+} quench of Fura-2 fluorescence was measured using photometry as described under "Experimental Procedures." a, dyspedic myotubes fail to respond to electrical pulse trains, whereas in b cell expressing C4958S-RyR1 rapidly respond to initiation and termination of the pulse train and the rate of Mn^{2+} entry (slope indicated by dashed lines) was dependent on the frequency of the pulses. Data shown are representative of measurements made on at least five separate cells.

where they engage a form of depolarization-triggered Ca^{2+} entry (ECCE) that is independent of SR store depletion.

To test whether the effects of serine substitution were specific to Cys⁴⁹⁵⁸ and Cys⁴⁹⁶¹, RyR1 proteins each possessing a cysteine point mutation (C3635S, C4872S, or C4882S) within the transmembrane assembly were constructed. Cys³⁶³⁵ is essential for the regulation of RyR1 by NO (49). Nevertheless myotubes expressing C3635S-RyR1 produced a rapid Ca^{2+} transient in response to depolarization with K^+ , and responded to caffeine in a dose-dependent manner (Fig. 5a). By contrast, myotubes expressing C4876S-RyR1 (Fig. 5b) or C4882S-RyR1 (data not shown) failed to respond to either stimulus.

Depolarization-triggered cation influx was indirectly measured by monitoring the quench of intracellular Fura-2 fluorescence by Mn^{2+} ,

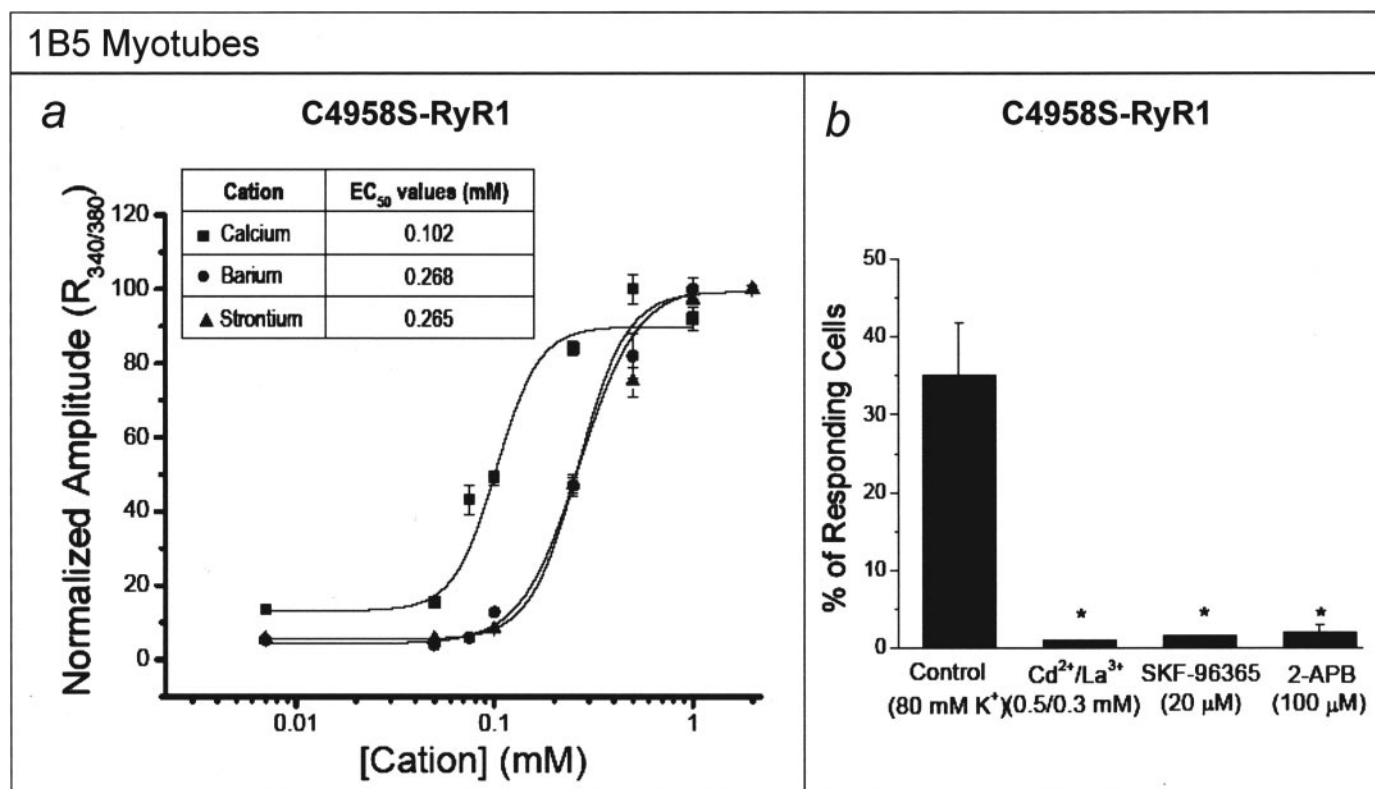


FIGURE 8. SOCC-like pharmacology of depolarization-induced Ca^{2+} influx exhibited by 1B5 myotubes expressing C4958S-RyR1. *a*, relationship between $[\text{cation}]_{\text{ex}}$ (Ca^{2+} , Sr^{2+} , and Ba^{2+}) and amplitude of cation entry produced by 80 mM K^+ applied to C4958S-RyR1 transduced 1B5 cells. EC₅₀ values (mM): 0.10 ± 0.007 for Ca^{2+} ; 0.26 ± 0.001 for Sr^{2+} and 0.26 ± 0.004 for Ba^{2+} . *b*, the effect of the cation channel blockers (1–2 min exposure) Cd^{2+} (0.5 mM) and La^{3+} (0.3 mM); and SOCC blockers $100 \mu\text{M}$ 2-APB and $20 \mu\text{M}$ SKF-96365 on the calcium response induced by 80 mM K^+ in 1B5 myotubes transduced with C4958S-RyR1 ($n = 327$ cells). The calcium response observed in the presence of $\text{Cd}^{2+}/\text{La}^{3+}$, 2-APB, and SKF-96365 for C4958S was significantly different (*, $p \leq 0.02$) from that observed in the absence of these channel blockers.

which enters cells via SOCC-like channels in the plasma membrane. Analysis of Mn^{2+} quench revealed that depolarization of dyspedic 1B5 or primary myotubes did not produce any detectable increase in the rate of quench of Fura-2 fluorescence from baseline (Fig. 6, *a* and *b*, 1st traces, respectively). In contrast, depolarization of 1B5 or primary myotubes expressing wild-type RyR1 resulted in rapid activation of Mn^{2+} entry evidenced by a significant increase in the rate of quench of Fura-2 fluorescence. (Fig. 6, *a* and *b*, 2nd traces). Thus, ECCE, a depolarization-induced entry of divalent cations via SOCC-like channels, was a fundamental property of myotubes expressing wild-type RyR1. Similarly, depolarization of myotubes expressing C4958S-RyR1 rapidly activated the influx of Mn^{2+} (Fig. 6, *a* and *b*, 3rd traces). The magnitude and rate of Mn^{2+} entry elicited by 80 mM K^+ with C4958S cells was very similar to that observed with myotubes expressing wild-type RyR1 that were pretreated with a channel blocking concentration of ryanodine (data not shown). Dyspedic myotubes had no Ca^{2+} release in response to trains of electrical pulses (Fig. 7*a*). Cells expressing either C4958S-RyR1 (Fig. 7*b*) or C4961S-RyR1 (data not shown) responded to electrical depolarization with an abrupt change in the rate of quench of Fura-2 fluorescence by Mn^{2+} entry, and the magnitude of the quench rate was directly related to the frequency of the stimulus (Fig. 7*b*).

The magnitude of the peak Ca^{2+} transient triggered by K^+ depolarization in C4958S-RyR1 expressing myotubes was dependent on Ca^{2+} concentration in the external medium, and exhibited a threshold and half-maximal amplitude (EC₅₀) of 50 and 102 μM , respectively (Fig. 8*a*). The relationship between driving force and cation selectivity of ECCE was further explored using substitutions of Ba^{2+} and Sr^{2+} in the extracellular medium. The EC₅₀ values obtained with Ba^{2+} and Sr^{2+} in the external medium were 268 and 265 μM , respectively (Fig. 8*a*). The rank

order of $\text{Ca}^{2+} > \text{Ba}^{2+} = \text{Sr}^{2+}$ for ECCE is consistent with the reported literature for I_{crac} and SOCC-type channels (45, 50, 51).

Cd^{2+} and La^{3+} have been shown to block ion conduction of a broad variety of Ca^{2+} channels. It was therefore expected that Cd^{2+} and La^{3+} (0.5 and 0.3 mM) would completely inhibit ECCE in 1B5 myotubes expressing C4958S-RyR1 (Fig. 8*b*). However, the presence of Cd^{2+} and La^{3+} has no significant effect on EC coupling elicited by K^+ depolarization in myotubes expressing wild type RyR1 (29). Organic blockers of SOCC include SKF-96356 and 2-APB. At concentrations shown to block SOCE in non-muscle cells, SKF-96356 (20 μM) or 2-APB (100 μM) completely blocked ECCE in myotubes expressing C4958S-RyR1 (Fig. 8*b*).

Whole Cell Responses to Long Depolarization in Myotubes Expressing C4958S-RyR1—ECCE appears to involve entry of divalent cations via SOCC-like ion channels, which should produce an inward ionic current. One might expect that 1) the ECCE-associated current would be small and/or activate relatively slowly, given that the ECCE-associated Ca^{2+} transient rises slowly, and 2) the ECCE-associated current should inactivate more slowly in cells expressing C4958S-RyR1 (where Ca^{2+} transients decay little during maintained depolarizations) than in cells expressing wild-type RyR1 (where Ca^{2+} transients decay rapidly during maintained depolarizations; see Fig. 4*d*). Fig. 9*a* illustrates whole cell Ca^{2+} currents elicited by strong (+30 mV) 2-s depolarizations. The total Ca^{2+} current (L-type current plus possible ECCE current) showed a similar extent of inactivation in cells expressing C4958S-RyR1 as in cells expressing wild-type RyR1 (Fig. 9*b*), suggesting that the contribution of ECCE current was too small to significantly alter inactivation of total current during a 2-s test pulse. Although there was little difference in the extent of inactivation, activation was more rapid for C4958S-RyR1 (Fig. 9*c*).

As another attempt to measure a current associated with ECCE, cells were directly depolarized from -80 mV to -20 mV. This test potential was selected because it was subthreshold for activation of L-type Ca^{2+} current but within the range of potentials expected to result from the elevated potassium concentrations (40 – 80 mM; Fig. 4c) and electrical pulse trains (Fig. 7b) sufficient to induce ECCE. Except for T-type Ca^{2+} current, no inward current was evident at -20 mV (Fig. 9). In particular, the average current near the end of the 6-s test pulse (5984 – 5994 ms) was -0.07 ± 0.23 ($n = 5$) and -0.03 ± 0.06 pA/pF ($n = 7$) for wild-type and C4958S-RyR1, respectively.

Store Depletion Also Activates Ca^{2+} Entry in Skeletal Myotubes—Depletion-activated Ca^{2+} entry mediated by activation of SOCCs in skeletal muscle has been previously described (17, 30). We tested whether or not this form of entry also exists in dyspedic 1B5 myotubes and those expressing wild-type and C4958S-RyR1 by depleting SR Ca^{2+} stores with 200 nM TG in EGTA-buffered external medium for 30 min. Upon subsequently elevating the external Ca^{2+} to 2 mM, a large sustained Ca^{2+} entry was observed in all three types of cells, consistent with activation of SOCE (Fig. 10, *a–c*, 1st traces). As expected, this sustained phase of the Ca^{2+} rise could be inhibited with either of the SOCE blockers 2-APB (52) or SKF-96365 (53) (Fig. 10, *a–c*, 2nd and 3rd traces, respectively). Thus, multiple pathways exist for the entry of extracellular calcium into skeletal muscle cells. Depolarization promotes Ca^{2+} entry via ECCE, T-type Ca^{2+} channels and L-type Ca^{2+} channels, whereas store depletion promotes entry via SOCE.

DISCUSSION

SOCE, a form of capacitative Ca^{2+} entry that involves activation of SOCCs, has recently been described in skeletal muscle cells. Activation of SOCCs has primarily been achieved by inducing non-physiological SR store depletion using SERCA pump inhibitors or repeated stimuli with caffeine in the presence of an external medium with a low Ca^{2+} concentration (17, 30). Evidence for a co-existing mechanism, termed ECCE, which has properties distinct from SOCE, was recently published (33). ECCE can be differentiated from SOCE in that: 1) ECCE produces entry of Ca^{2+} in response to physiological depolarizing stimuli, whereas SOCE in muscle is inhibited by depolarization (17), 2) activation of ECCE does not appear to require appreciable store depletion, and 3) ECCE requires interactions among three different Ca^{2+} channels, a SOCC-like channel, the α_{1S} -DHPR and RyR1 (33), and accordingly ECCE is absent in dyspedic, RyR-null, myotubes (Fig. 7) and dysgenic, α_{1S} -DHPR-null, myotubes (data not shown), whereas SOCE is preserved in these cell types (Fig. 10).

In the present study, we report that substitution of RyR1 cysteines 4958 or 4961 with serine disables activation of SR Ca^{2+} release in response to plasma membrane depolarization or to direct RyR1 agonists such as caffeine. However, C4958S-RyR1 and C4961S-RyR1 are properly targeted to peripheral junctions and couple with α_{1S} -DHPR, as demonstrated by restoration of a significant density of L-type Ca^{2+} current. Moreover, in both primary and 1B5 myotubes, the cysteine-mutant RyRs are able to support depolarization-induced Ca^{2+} entry via ECCE, which cannot, therefore, be secondary to depolarization-induced release of the SR Ca^{2+} store. Indeed, application of SERCA pump blockers provides direct evidence that the SR store is statically replete in myotubes expressing C4958S-RyR1 (Fig. 2).

The importance of RyR1 conformation for ECCE is emphasized by the observation that Ca^{2+} transients in myotubes expressing C4958S-RyR1 are sustained during K^+ depolarizations lasting many seconds, whereas those in myotubes expressing wild-type RyR1 inactivate rapidly (Fig. 4d). Thus, the substitution of cysteines within the TXCFICG motif

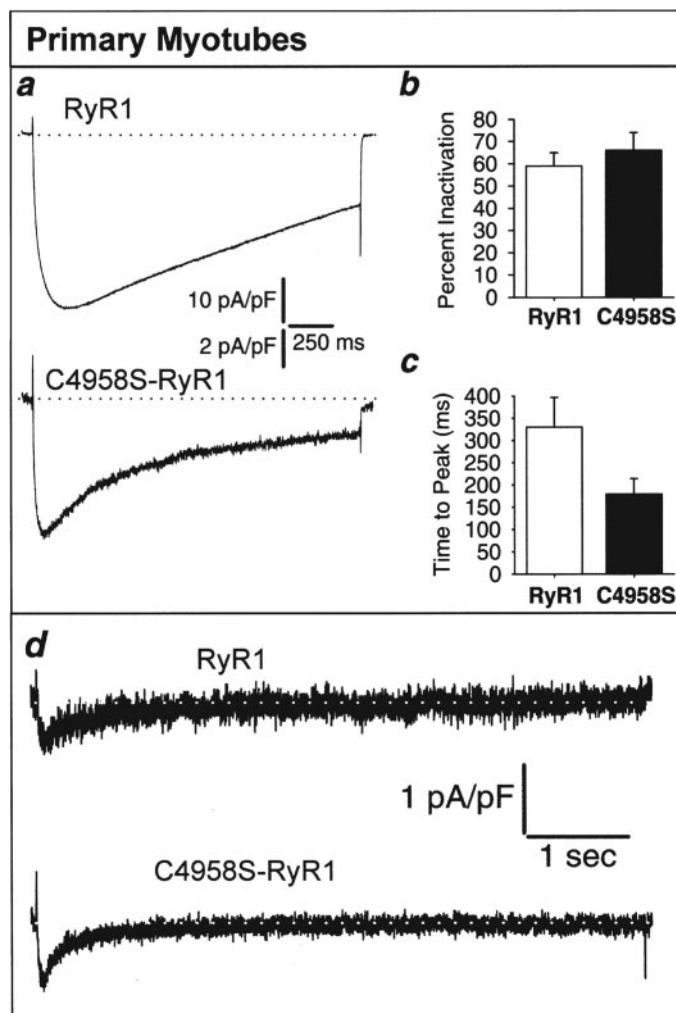


FIGURE 9. Activation and inactivation of Ca^{2+} currents in myotubes expressing wild-type or C4958S-RyR1. *a*, representative Ca^{2+} currents for a 2-s test pulse to $+30$ mV are shown for myotubes expressing wild-type (top) or C4958S-RyR1 (bottom). Note that the trace for C4958S-RyR1 is shown at increased vertical gain to allow easier kinetic comparison with wild-type RyR1. *b*, average inactivation, calculated as $100 \times (1 - I_{2s}/I_{\text{peak}})$, was not significantly different ($p > 0.5$) between wild-type RyR1 (white bars; $n = 12$) and C4958S-RyR1 (black bars; $n = 16$). *c*, time to peak current for C4958S-RyR1 (black bars; $n = 16$) was significantly shorter ($p < 0.05$) than for wild-type RyR1 (white bars; $n = 12$). The traces used from each cell to calculate the averages in *b* and *c* were recorded at the voltage that produced the maximal Ca^{2+} current (range $+20$ to $+40$ mV). *d*, lack of sustained inward, whole cell current during prolonged, weak depolarizations. Representative traces are shown for 6-s depolarizations from -80 to -20 mV applied to primary myotubes expressing wild-type (top) or C4958S-RyR1 (bottom), where the dotted line indicates the zero current level. The transient Ca^{2+} current during the initial ~ 300 ms of the test pulse arises from T-type channels, which were inactivated by a prior pre-pulse in the records illustrated in Fig. 1 and in *a* above.

results in an RyR1 conformation resembling that stabilized by exposure of the wild-type RyR1 to $\sim 10^{-4}$ M ryanodine, which has the similar effect of both blocking EC coupling and causing ECCE to be sustained during long depolarizations (33). This sort of ryanodine treatment produces a large conformational change in the DHPR-RyR1 junctional complex, causing a 2-nm reduction in the distance between adjacent particles within tetrads (25). Because tetrads represent groups of four α_{1S} -DHPRs coupled to the four subunits of RyR1, it is tempting to speculate that this large conformational change propagated from RyR1 to the DHPRs is also involved in the altered behavior of the Ca^{2+} entry pathway activated during ECCE.

A number of structural elements have been identified as contributing to conformational coupling between α_{1S} -DHPR and RyR1. For skeletal-type EC coupling, significant structures include the C-terminal of β_{1a}

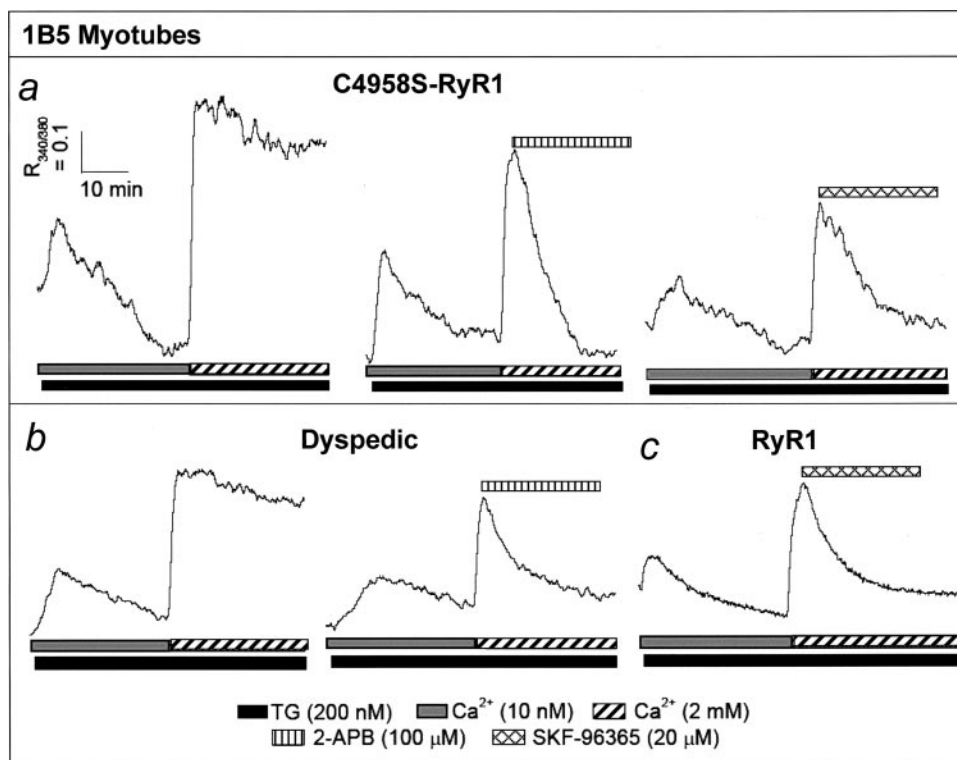


FIGURE 10. SR depletion activated SOCC in 1B5 myotubes. Representative traces illustrating capacitative calcium entry in 1B5 myotubes transduced with C4958S-RyR1 (*a*, $n = 30$ cells), dyspedic 1B5 myotubes (*b*, $n = 45$ cells), and 1B5 myotubes transduced with wild-type RyR1 ($n = 20$ cells). To elicit capacitative calcium entry, intracellular stores were depleted by a 20–30 min application of 200 nM thapsigargin (TG) in an external solution containing 10 nM calcium. Subsequent elevation of external calcium to 2 mM induced sustained capacitative calcium entry. The capacitative calcium entry was blocked by the addition of the SOCC blockers 2-APB (100 μM , 2-min exposure) and SKF-96365 (20 μM , 2-min exposure).

(54) and a segment of the α_{15} II-III loop (residues 720–765) (39). This same α_{15} II-III loop segment is also important for the retrograde enhancement of L-type Ca^{2+} current (26, 55) and for the RyR1-dependent organization of DHPRs into tetrads (56). Several regions of RyR1 have been shown to contribute essential elements of structure necessary for skeletal-type EC coupling (29, 57), the retrograde enhancement of L-type Ca^{2+} current (39) and the organization of DHPRs into tetrads (27). It will be valuable to determine to what extent ECCE depends upon the same DHPR and RyR structures. However, it already seems clear that the pathway producing ECCE diverges in part from that of EC coupling. As one obvious example, replacing either Cys⁴⁹⁵⁸ or Cys⁴⁹⁶¹ with serine ablates EC coupling via RyR1 but enhances ECCE as a consequence of slowed inactivation and deactivation. Importantly, enhancement of ECCE is not a consequence of all RyR1 mutations that impair EC coupling. When Glu⁴⁰³² is mutated to Ala⁴⁰³² there is a ~75% reduction in EC coupling as indicated by whole cell voltage clamp analysis of Ca^{2+} transients (58). Here we examined three additional cysteine mutations within the RyR1 transmembrane assembly (C3635S, C4876S, and C4882S). None of these produced the phenotype observed with C4958S or C4961S (*i.e.* complete lack of orthograde signaling because of an RyR1 dysfunction, but preserved retrograde signaling with both DHPR and ECCE).

Two chief features reported here for ECCE in myotubes expressing C4958S-RyR1 are indistinguishable from those of ECCE in wild-type myotubes (33). First, Ca^{2+} entry via ECCE is fully inhibited by brief application of micromolar SKF-96365 and 2-APB. Second, the entry pathway is permeable to Mn^{2+} and displays cation permeability with a rank order of $\text{Ca}^{2+} > \text{Ba}^{2+} = \text{Sr}^{2+}$. These properties suggest that Ca^{2+} entry via ECCE involves a channel with properties like those of the channels underlying I_{crac} or SOCE (45, 50, 51). Direct, whole cell measurements of the current associated with SOCE have been reported for a number of cell types (59). However, whole cell measurements failed to reveal a current associated with ECCE in myotubes expressing C4958S-RyR1 (Fig. 9) even though ECCE was clearly observed in intact myo-

tubes stimulated with electrical pulse trains using the Mn^{2+} quench method (Fig. 7). At least three possibilities could explain this failure. One possible explanation is that rupturing the cell membrane led to a loss of cytoplasmic components necessary for ECCE. However, the whole cell conditions we used were generally comparable to those used by others to measure SOCE currents. A second possibility is that the ECCE current was too small to be detected. In regard to this possibility, it is necessary to point out that ECCE was restored by expression in dysgenic myotubes of “SkEIIIK” (33), a mutated α_{15} -DHPR, which does not conduct inward Ca^{2+} current but does function as a voltage sensor for EC coupling (60). After treatment with 0.5 mM ryanodine (to block EC coupling and enhance ECCE), the Ca^{2+} transients produced by K^{+} depolarization were of similar size in myotubes expressing wild-type or SkEIIIK α_{15} -DHPR,⁵ which would seem to indicate that L-type Ca^{2+} current via the DHPR produces a negligible change in cytoplasmic Ca^{2+} compared with that caused by ECCE. If this were correct, then one would expect the current associated with ECCE to be substantially larger than the L-type Ca^{2+} current and thus easily measurable. A third possibility, therefore, is that the entry of Ca^{2+} associated with ECCE is not electrogenic as would occur, for example, if the entering Ca^{2+} were exchanged in an electroneutral fashion for internal cations.

The functional changes caused by either the C4958S or C4961S mutations may result from alterations in the conformational stability of the RyR1 tetramer. The dysfunctional RyR1 conformation observed in the present study may be a result of either a loss of native disulfide linkages, formation of aberrant disulfide linkages, or both. In this regard, several classes of cysteine residues within RyR1 are essential for maintaining the functional integrity of the channel complex. Of the 100 cysteine residues in each RyR1 subunit, 25–50 are thought to be free (not disulfide bonded) and these fall into 3–4 classes based on their reactivity (49, 61–63). Several thioether adducts of 7-diethylamino-3-(4'-male-

⁵ G. Cherednichenko and I. N. Pessah, unpublished data.

imidylphenyl)-4-methylcoumarin (CPM; Refs. 61 and 64) with hyper-reactive RyR1 cysteines were recently identified using mass spectrometry (36). In addition to Cys³⁶³⁵, the site of nitrosylation (49), six additional cysteines (1040, 1303, 2436, 2565, 2606, and 2611) were identified as hyper-reactive, and may contribute to redox regulation of the RyR1 complex (36, 65, 66). Because neither cysteine within the TXCFICG motif was detected under labeling conditions that select the most reactive CPM-thioether adducts, it is possible that in the native (functional) channel these cysteines are disulfide-bonded (oxidized). If this were the case, it would suggest that the loss of disulfide bond pairing after serine substitution for either Cys⁴⁹⁵⁸ or Cys⁴⁹⁶¹ could account for the disabling of RyR1 channel function. This interpretation is supported by the fact that Cys⁴⁹⁵⁸ and Cys⁴⁹⁶¹ conform to a CXXC motif that has been identified in many proteins as controlling formation, isomerization, and reduction of disulfide bonds, in addition to other redox functions (37, 67). Recent studies revealed the existence of natural homologues of CXXC-containing proteins, in which the C-terminal or N-terminal Cys in the CXXC motif is replaced with serine (*i.e.* CXXS or SXXC, respectively), which causes the formation of alternative intra- or intermolecular disulfide bonds, stabilizes alternative conformations, and expands the biochemical functions of the protein (68, 69). It is therefore reasonable that the Cys⁴⁹⁵⁸ and Cys⁴⁹⁶¹ might serve to maintain a functional three-dimensional structure of the RyR1 channel by establishing precise disulfide bond linkages, and that substitution with serine promotes alternative disulfide linkages either within the RyR1 tetramer or to accessory proteins within the channel complex. In this regard, the presence of strong reductants like dithiothreitol were shown to partially protect the channel from assuming the persistent conformation induced by micromolar ryanodine, implicating the rearrangement of one or more sulfhydryl/disulfide linkages as involved in stabilizing the inactive channel conformation (70), a conformation which the present study shows to be functionally mimicked by C4958S and C4961S.

In summary, we have shown that ECCE is not dependent on a rise in cytoplasmic Ca²⁺ and does not require any store depletion. ECCE co-exists with classic SOCE in myotubes, although only activation of ECCE is absolutely dependent on expression of both RyR1 and α_{15} -DHP. Furthermore the characteristics of Ca²⁺ entry triggered by ECCE is highly dependent on the conformation of RyR1 as evidenced by the changes in its inactivation/deactivation kinetics brought on by either ryanodine (33) or by the mutation of either of two highly invariant cysteine residues (4958 and 4961) located in the TXCFICG motif (present findings).

REFERENCES

- Berridge, M. J. (1998) *Neuron* **21**, 13–26
- Berridge, M. J., Lipp, P., and Bootman, M. D. (2000) *Nat. Rev. Mol. Cell Biol.* **1**, 11–21
- Nakai, J., Dirksen, R. T., Nguyen, H. T., Pessah, I. N., Beam, K. G., and Allen, P. D. (1996) *Nature* **380**, 72–75
- Chavis, P., Fagni, L., Lansman, J. B., and Bockaert, J. (1996) *Nature* **382**, 719–722
- Kiselyov, K. I., Shin, D. M., Wang, Y., Pessah, I. N., Allen, P. D., and Muallem, S. (2000) *Mol. Cell* **6**, 421–431
- Chavis, P., Ango, F., Michel, J. M., Bockaert, J., and Fagni, L. (1998) *Eur. J. Neurosci.* **10**, 2322–2327
- Perez, G. J., Bonev, A. D., Patlak, J. B., and Nelson, M. T. (1999) *J. Gen. Physiol.* **113**, 229–238
- Putney, J. W., Jr. (2004) *Trends Cell Biol.* **14**, 282–286
- Parekh, A. B. (2003) *J. Physiol.* **547**, 333–348
- Parekh, A. B., and Penner, R. (1997) *Physiol. Rev.* **77**, 901–930
- Smani, T., Zakharov, S. I., Csutora, P., Leno, E., Trepakova, E. S., and Bolotina, V. M. (2004) *Nat. Cell Biol.* **6**, 113–120
- Bakowski, D., Burgoyne, R. D., and Parekh, A. B. (2003) *J. Physiol.* **553**, 387–393
- Bezzides, V. J., Ramsey, I. S., Kotecha, S., Greka, A., and Clapham, D. E. (2004) *Nat. Cell Biol.* **6**, 709–720
- Putney, J. W., Jr., Broad, L. M., Braun, F. J., Lievreumont, J. P., and Bird, G. S. (2001) *J. Cell Sci.* **114**, 2223–2229
- Taylor, C. W. (2002) *Cell* **111**, 767–769
- Uehara, A., Yasukochi, M., Imanaga, I., Nishi, M., and Takeshima, H. (2002) *Cell Calcium* **31**, 89–96
- Kurebayashi, N., and Ogawa, Y. (2001) *J. Physiol.* **533**, 185–199
- Kiselyov, K., Xu, X., Mozhayeva, G., Kuo, T., Pessah, I., Mignery, G., Zhu, X., Birnbaumer, L., and Muallem, S. (1998) *Nature* **396**, 478–482
- Launikonis, B. S., Barnes, M., and Stephenson, D. G. (2003) *Proc. Natl. Acad. Sci. U. S. A.* **100**, 2941–2944
- Elliott, A. C. (2001) *Cell Calcium* **30**, 73–93
- Fleig, A., Takeshima, H., and Penner, R. (1996) *J. Physiol.* **496**, 339–345
- Avila, G., and Dirksen, R. T. (2000) *J. Gen. Physiol.* **115**, 467–480
- Avila, G., O'Connell, K. M., Groom, L. A., and Dirksen, R. T. (2001) *J. Biol. Chem.* **276**, 17732–17738
- Lorenzon, N. M., Grabner, M., Suda, N., and Beam, K. G. (2001) *Arch Biochem. Biophys.* **388**, 13–17
- Paolini, C., Fessenden, J. D., Pessah, I. N., and Franzini-Armstrong, C. (2004) *Proc. Natl. Acad. Sci. U. S. A.* **101**, 12748–12752
- Grabner, M., Dirksen, R. T., Suda, N., and Beam, K. G. (1999) *J. Biol. Chem.* **274**, 21913–21919
- Protasi, F., Paolini, C., Nakai, J., Beam, K. G., Franzini-Armstrong, C., and Allen, P. D. (2002) *Biophys. J.* **83**, 3230–3244
- Perez, C. F., Mukherjee, S., and Allen, P. D. (2003) *J. Biol. Chem.* **278**, 39644–39652
- Perez, C. F., Voss, A., Pessah, I. N., and Allen, P. D. (2003) *Biophys. J.* **84**, 2655–2663
- Ma, J., and Pan, Z. (2003) *Cell Calcium* **33**, 375–384
- Thastrup, O., Cullen, P. J., Drobak, B. K., Hanley, M. R., and Dawson, A. P. (1990) *Proc. Natl. Acad. Sci. U. S. A.* **87**, 2466–2470
- Seidler, N. W., Jona, I., Vegh, M., and Martonosi, A. (1989) *J. Biol. Chem.* **264**, 17816–17823
- Cheredinchenko, G., Hurne, A. M., Fessenden, J. D., Lee, E. H., Allen, P. D., Beam, K. G., and Pessah, I. N. (2004) *Proc. Natl. Acad. Sci. U. S. A.* **101**, 15793–15798
- Pessah, I. N., Kim, K. H., and Feng, W. (2002) *Front Biosci.* **7**, a72–79
- Hamilton, S. L., and Reid, M. B. (2000) *Antioxid. Redox Signal.* **2**, 41–45
- Voss, A. A., Lango, J., Ernst-Russell, M., Morin, D., and Pessah, I. N. (2004) *J. Biol. Chem.* **279**, 34514–34520
- Fomenko, D. E., and Gladyshev, V. N. (2003) *Biochemistry* **42**, 11214–11225
- Wang, Y., Fraefel, C., Protasi, F., Moore, R. A., Fessenden, J. D., Pessah, I. N., DiFrancesco, A., Brakefield, X., and Allen, P. D. (2000) *Am. J. Physiol. Cell Physiol.* **278**, C619–626
- Nakai, J., Sekiguchi, N., Rando, T. A., Allen, P. D., and Beam, K. G. (1998) *J. Biol. Chem.* **273**, 13403–13406
- Moore, R. A., Nguyen, H., Galceran, J., Pessah, I. N., and Allen, P. D. (1998) *J. Cell Biol.* **140**, 843–851
- Rando, T. A., and Blau, H. M. (1994) *J. Cell Biol.* **125**, 1275–1287
- Jurman, M. E., Boland, L. M., Liu, Y., and Yellen, G. (1994) *BioTechniques* **17**, 876–881
- Grabner, M., Dirksen, R. T., and Beam, K. G. (1998) *Proc. Natl. Acad. Sci. U. S. A.* **95**, 1903–1908
- O'Brien, J. J., Feng, W., Allen, P. D., Chen, S. R., Pessah, I. N., and Beam, K. G. (2002) *Biophys. J.* **82**, 2428–2435
- Clementi, E., Scheer, H., Zacchetti, D., Fasolato, C., Pozzan, T., and Meldolesi, J. (1992) *J. Biol. Chem.* **267**, 2164–2172
- Merritt, J. E., Jacob, R., and Hallam, T. J. (1989) *J. Biol. Chem.* **264**, 1522–1527
- Rink, T. J. (1990) *FEBS Lett.* **268**, 381–385
- Protasi, F., Franzini-Armstrong, C., and Allen, P. D. (1998) *J. Cell Biol.* **140**, 831–842
- Sun, J., Xu, L., Eu, J. P., Stamler, J. S., and Meissner, G. (2001) *J. Biol. Chem.* **276**, 15625–15630
- Barritt, G. J. (1999) *Biochem. J.* **337**, 153–169
- Jacob, R. (1990) *J. Physiol.* **421**, 55–77
- Diver, J. M., Sage, S. O., and Rosado, J. A. (2001) *Cell Calcium* **30**, 323–329
- Merritt, J. E., Armstrong, W. P., Benham, C. D., Hallam, T. J., Jacob, R., Jaxa-Chamiec, A., Leigh, B. K., McCarthy, S. A., Moores, K. E., and Rink, T. J. (1990) *Biochem. J.* **271**, 515–522
- Beurg, M., Ahern, C. A., Vallejo, P., Conklin, M. W., Powers, P. A., Gregg, R. G., and Coronado, R. (1999) *Biophys. J.* **77**, 2953–2967
- Wilkens, C. M., Kasielke, N., Flucher, B. E., Beam, K. G., and Grabner, M. (2001) *Proc. Natl. Acad. Sci. U. S. A.* **98**, 5892–5897
- Takekura, H., Paolini, C., Franzini-Armstrong, C., Kugler, G., Grabner, M., and Flucher, B. E. (2004) *Mol. Biol. Cell* **15**, 5408–5419
- Nakai, J., Tanabe, T., Konno, T., Adams, B., and Beam, K. G. (1998) *J. Biol. Chem.* **273**, 24983–24986
- Fessenden, J. D., Chen, L., Wang, Y., Paolini, C., Franzini-Armstrong, C., Allen, P. D., and Pessah, I. N. (2001) *Proc. Natl. Acad. Sci. U. S. A.* **98**, 2865–2870
- Parekh, A. B., and Putney, J. W., Jr. (2005) *Physiol. Rev.* **85**, 757–810
- Dirksen, R. T., and Beam, K. G. (1999) *J. Gen. Physiol.* **114**, 393–403
- Liu, G., Abramson, J. J., Zable, A. C., and Pessah, I. N. (1994) *Mol. Pharmacol.* **45**, 189–200

RyR1 Cys Mutations Unmask ECCE

62. Aghdasi, B., Zhang, J. Z., Wu, Y., Reid, M. B., and Hamilton, S. L. (1997) *J. Biol. Chem.* **272**, 3739–3748
63. Dulhunty, A., Haarmann, C., Green, D., and Hart, J. (2000) *Antioxid. Redox Signal.* **2**, 27–34
64. Liu, G., and Pessah, I. N. (1994) *J. Biol. Chem.* **269**, 33028–33034
65. Feng, W., Liu, G., Allen, P. D., and Pessah, I. N. (2000) *J. Biol. Chem.* **275**, 35902–35907
66. Xia, R., Stangler, T., and Abramson, J. J. (2000) *J. Biol. Chem.* **275**, 36556–36561
67. Holmgren, A. (2000) *Biofactors* **11**, 63–64
68. Fomenko, D. E., and Gladyshev, V. N. (2002) *Protein Sci.* **11**, 2285–2296
69. Anelli, T., Alessio, M., Mezghrani, A., Simmen, T., Talamo, F., Bachi, A., and Sitia, R. (2002) *EMBO J.* **21**, 835–844
70. Zimanyi, L., Buck, E., Abramson, J. J., Mack, M. M., and Pessah, I. N. (1992) *Mol. Pharmacol.* **42**, 1049–1057
71. Airey, J. A., Beck, C. F., Murakami, K., Tanksley, S. J., Deerinck, T. J., Ellisman, M. H., and Sutko, J. L. (1990) *J. Biol. Chem.* **265**, 14187–14194

